

# Investigation of the Effect of Drilling Induced Delamination and Tool Wear on Residual Strength in Polymer Nanocomposites

**R. Pramod**

Assistant Professor  
Mechanical Engineering Department  
Amrita School of Engineering  
Bengaluru Campus  
Amrita Vishwa Vidyapeetham  
India

**Veeresh Kumar G.B.**

Assistant Professor  
Mechanical Engineering Department  
National Institute of Technology  
Andhra Pradesh, Tadepalligudem  
Andhra Pradesh  
India

**Basavarajappa S.**

Professor  
Department of Mechanical Engineering  
University B.D.T College of Engineering  
V.T.U, Davanagere  
India

*Drilling-induced delamination, fractures, debonding, tool wear, and matrix fuzzing all reduce the residual strength of polymer composites. The novelty of the present studies lies in incorporating nano-fillers Graphene and Montmorillonite Clay at a 2% weight percentage for the toughening matrix to minimize drilling-induced residual stresses and tool wear. Combining the matrix's thermal and mechanical properties with fibers reduces fibrous composite macro and micro residual stresses. Interlaminar shear strength rose by 16%–23% and fracture toughness by 22% using nanofillers, minimizing drilling-induced crack delamination and composite tensile strength deterioration. Nanofillers increased hole laminate tensile strength retention and time to failure. Tool wear and delamination factors rose at the hole exit with increased drilled holes but improved at the entry by 16%. This study shows the intricate link between composite material composition, process variables, and structural integrity in drilling-exposed composites.*

**Keywords:** Delamination, Delamination factor, residual stress, tool wear, Graphene, Montmorillonite Clay.

## 1. INTRODUCTION

Polymer matrix composites (P.M.C.s) have been widely used in many sectors, such as military, space, marine, sports, aviation, and vehicles, for a significant period. Their extensive use may be due to various elements, including a good ratio of strength to weight, toughness, cost-effectiveness, ease of processing, simplicity in production, and remarkable longevity. These materials have become essential for satisfying numerous industries' broad and demanding demands and have established themselves as crucial components in the manufacturing industry. Their appeal stems from their advantageous strength-to-weight ratio, toughness, cost-effectiveness, simplicity of processing, ease of manufacture, and durability. Several studies have concentrated on improving the toughness of matrices by integrating various fillers and using matrix-blending procedures [1,2].

Studies have investigated how the choice of drill tool materials, drill geometry, and drilling mechanics affect the quality of holes in P.M.C.s. According to the literature, delamination often happens on both sides of the hole at the entrance and exit planes of the workpiece [3]. Hocheng and Tsao conducted a study to examine the impact of several types of drill bits, including step drills, saw drills, twist drills, core drills, and candlestick drills, on the occurrence of delamination [4-6]. Many

researchers have explored the possibility of a predrilled hole, as a pilot hole diminishes the significant thrust force and examined the impact of the chisel edge on delamination. Several assessment techniques have been used to evaluate delamination, including computed tomography, the C-Scan methodology, digital photography, optical microscopy, and image processing [7]. Multiple trials have emphasized the pivotal significance of tool geometry in minimizing delamination [8], with research indicating that augmenting the quantity of cutting edges in the drill tool diminishes delamination [9].

Multiple studies have demonstrated a connection between the wearing down of tools and the occurrence of delamination. This highlights the need to monitor tool wear in real-time. The primary form of tool wear discovered was flank wear on the drill surfaces, and a decrease in the chisel edge led to a reduction in wear. The presence of inefficient chip extraction methods was shown to be associated with increased tool deterioration [10,11]. The study used experimental design methodologies to identify relationships between drilling parameters, delamination variables, specific cutting pressure, and feed rate [12].

Using laminates in drilling helps minimize delamination but also poses difficulties in attaining ideal machining conditions for two distinct materials simultaneously [13]. Aluminum (Al) stacks are often used, and various drill tool designs have been tested to evaluate the crucial thrust force and Torque during drilling [14,15]. Palanikumar et al. conducted an experimental study to examine the surface roughness of drilled holes in GFRP composites [16]. Basavarajappa et al. used simulated annealing methods to investigate

Received: April 2024, Accepted: September 2024.

Correspondence to: Dr. Veeresh Kumar G B,  
National Institute of Technology-Andhra Pradesh,  
Tadepalligudem, Andhra Pradesh, India.

E-mail: veereshkumargb@nitandhra.ac.in

doi: 10.5937/fme2404573P

the impact of machining conditions on the delamination factor, specific cutting coefficient, and surface roughness [17].

According to the literature, using appropriate filler materials in the polymer matrix may increase toughness, enhance machinability, and decrease specific cutting pressure [18-19]. Nevertheless, research indicates that the bearing strength of composites decreases as the reinforcement level increases. Nanofillers have superior performance in enhancing the toughness of the matrix compared to micro-fillers. However, hybrid nanofillers lead to the clumping together of particles and do not provide promising outcomes in strengthening the matrix [20]. An increasing interest exists in examining the machining mechanics of nano polymer composites and investigating their possible applications in aerospace and automotive applications. Insufficient work has been carried out in drilling nanocomposites, residual strength estimation under drilling of laminates, and tool wear behaviour under nanocomposites drilling. The present study examines how nanoparticle-reinforced matrices, with nano clay and graphene nanoplatelets, affect drilled hole quality. The study evaluates tool wear, residual stresses, and critical thrust force reduction on the delamination factor [Df]. Image processing estimates the delamination factor. These data show how much nanoparticle toughening enhances drilling performance compared to virgin matrix composites. This research analyzes how adding 2% graphene and montmorillonite clay nano-fillers to polymer composites improves their capacity to endure drilling residual stresses and tool wear. This study optimizes the matrix's mechanical and thermal properties, reduces fibrous composite residual stresses, and improves interlaminar shear strength, fracture toughness, and residual tensile strength. In addition, this research will examine how nano-fillers reduce drilling tool wear and delamination.

## 2. MATERIALS AND METHODOLOGY

The manufacturing process of Polymer Matrix Composite (P.M.C.) laminate included procuring 200 GSM unidirectional E-glass fibers from Marqtech in Bengaluru. The Araldite LY556 resin and Aradur HY951 hardener have been chosen as the matrix. Around 5% of hardener was used, leading to an exothermic reaction. The system's responsiveness may be modified to suit certain processing and curing conditions. The creation of nano-PMCs consists of two primary steps: a) managing the dispersion of nano-filler materials within the epoxy resin system, and b) manufacturing using the Handlay Process. The additives used in preparing P.M.C.s consisted of Montmorillonite clay, Nanomer® I.44P, and Nanomer® clay sourced from Sigma-Aldrich. The Nanomer® clay consisted of 35-45 wt.% dimethyl dialkyl (C14-C18) amine. It had an average particle size of  $\leq 20 \mu\text{m}$ , a bulk density ranging from 200-500  $\text{kg/m}^3$ , an aspect ratio of 200-1000, and an average surface area of 780  $\text{m}^2/\text{g}$ . The amine-functionalized graphene powder was acquired from Sigma-Aldrich. It had a specific gravity of 2-2.25  $\text{g/cc}$ , a bulk density of 0.2-0.4  $\text{g/cc}$ , and a surface area of 750  $\text{m}^2/\text{g}$ . The nanofillers create a complex structure

when dispersed in the epoxy matrix, which slows down the pace at which they can penetrate. The chemical Maleic Anhydride ( $\text{C}_4\text{H}_2\text{O}_3$ ) acquired from Sigma-Aldrich is a surface modifying agent. This aims to reduce the tension between distinct interfaces and improve the ability of different phases to mix and get the desired characteristics [21]. The Nanoparticles were mixed with styrene monomer and then introduced into the epoxy resin. The mixture was swirled by hand and then agitated at a temperature of 60 °C using a REMI magnetic stirrer for 80-120 minutes at an 800-1250 rpm speed. Afterwards, the combination was subjected to sonication using an Oscar Ultrasonics Sonicator running at 2.5 kHz for 60 minutes. A pulse interval of two seconds was used to reduce particle clumping and guarantee uniform dispersion inside the matrix. Composite laminates, 6 mm thick, were produced using a manual layup method and underwent a three-hour curing process in a hot air convection oven at 80 C. The production of Nanoclay-reinforced epoxy composites and Graphene-reinforced epoxy composites included the addition of 2% reinforcement. Three types of laminates were manufactured: Base Composites (B.C.) without any reinforcement, Nano clay reinforced composites (N.C.) with a 2 wt.% reinforcement, and Graphene reinforced composites (G.R.) with a 2 wt.% reinforcement. Particle agglomeration occurred when the proportion of reinforcement approached 2 wt.%, as shown in several articles [22-23].

The tensile strength [ $\sigma_T$ ] was measured using the Instron Universal Testing equipment following the ASTM 3039/ISO 527-4 standard. The interlaminar shear stress [ILSS] test followed the ASTM D2344 standard. The short-beam shear test method was used. The flexural strength [F.S.] was evaluated following the ASTM standard D790-10. We measured the density in accordance with the ASTM D792 standard. Table 1 displays the mechanical properties of the composites produced.

**Table 1. Fabricated P.M.C.'s mechanical properties.**

Composite Laminates	$\rho$ (g/cc)	$\sigma_T$ (MPa)	F.S. (MPa)	ILSS (MPa)	Fracture Toughness $\text{MPa/m}^{1/2}$ [ISO 6603-1]
Base Composite [BC]	1.87	328.6	198.46	21.58	0.964
Nano clay reinforced [NC]	1.864	408.6	278.89	25.36	1.248
Graphene reinforced [GR]	1.862	423.5	318.64	28.86	1.324

### 2.1 FTIR and XRD analysis

The nanocomposites were analyzed using Shimadzu Fourier transform infrared spectroscopy (FTIR) to confirm the presence of several functional peaks in the nanocomposites. Figure 1 displays the FTIR spectroscopy results of the Epoxy and Epoxy toughened with Nanoclay-reinforced nanocomposite. The absorption

bands can be witnessed in the spectrums of FTIR at 3430–2990  $\text{cm}^{-1}$ , N-H stretching and bending at 1632–1566  $\text{cm}^{-1}$ , and  $\text{CH}_2$  and  $\text{CH}_3$  absorption at 3015  $\text{cm}^{-1}$  and 2944  $\text{cm}^{-1}$ .

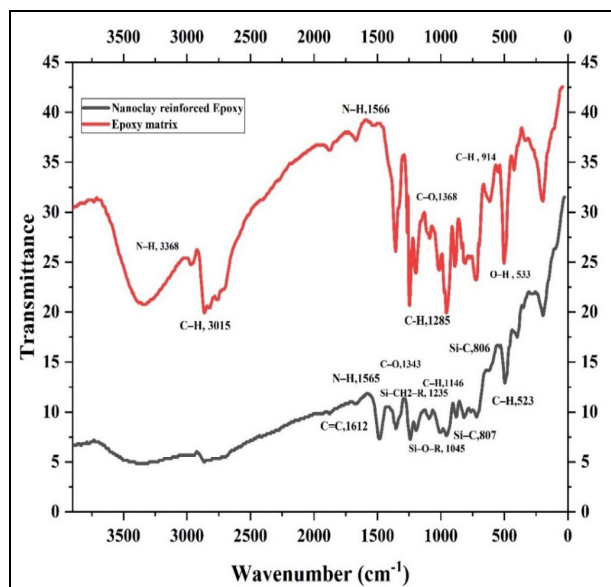


**Figure 1.** FTIR spectroscopy of the Epoxy and Epoxy toughened with Nanoclay.

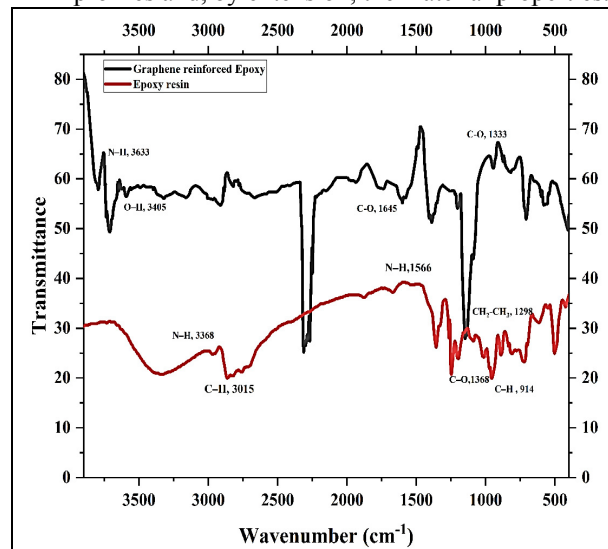
After introducing the hardener into the resin, the reaction yields bending of C-H and O-H deformation out of the plane in regions 1285–986  $\text{cm}^{-1}$  and 533  $\text{cm}^{-1}$ , respectively, with vibrations coupled in regions 560–855  $\text{cm}^{-1}$ . An aromatic type of structure is witnessed. Toughening of the matrix is achieved by the reaction of Epoxy with the Silicon present in Nanoclay with asymmetric stretching of Si-O-R and Si-O-C. It is evident at the spectrum range 1200–950  $\text{cm}^{-1}$  with an additional Si-CH<sub>2</sub>-R around 1230–1190  $\text{cm}^{-1}$ . The reaction of Silicon with O and C in Epoxy can be seen around 806  $\text{cm}^{-1}$  [24–25].

Figure 2 shows the bonding between the Graphene and Epoxy resin with stretching of vinyl ether in an asymmetric and symmetric mode at 1225.5  $\text{cm}^{-1}$  and 815.6  $\text{cm}^{-1}$ , respectively. The carbonyl group is observed at 1645  $\text{cm}^{-1}$  due to H-bonding between Epoxy and Graphene. Further, stretching is observed in the 3400–3700  $\text{cm}^{-1}$  N-H and O-H range.

The X-ray diffraction (XRD) profiles of Epoxy, Epoxy toughened with Nanoclay, and Epoxy toughened with Graphene nanoplatelets were acquired using the Rigaku Ultima series X-ray Diffractometer. The measurements were performed at a scan rate of 0.05 per second, using Cu-K  $\alpha$  radiation with a wavelength ( $\lambda$ ) of 0.15406 nm. The observed patterns covered a range of angles from 1° to 30°, with a scanning rate of 0.15 degrees per minute [26–27]. Bragg's Law calculates the distance ( $d$ ) between the planes of an atomic lattice. The findings indicated that as the degree of cohesive layer stacking of the clay increased, there was a corresponding increase in peak expansion and greater strength seen at larger X-ray angles [28–29].

This analytical approach provided valuable insights into the structural characteristics and interactions within the examined epoxy composites, shedding light on the

influence of nanoclay and graphene nanoplatelets on the XRD profiles and, by extension, the material properties.



**Figure 2.** FTIR spectroscopy of the Epoxy and Epoxy toughened with Graphene.

The XRD patterns of the Nanoclay are shown in Figure 3. As a result of intercalation between the Nanoclay and Epoxy resin, a peak is observed at  $2\theta = 4.3^\circ$  corresponding to a basal spacing with 2.114 Å. These peaks are not observed in the Nanoclay-reinforced resin because of the exfoliation of the nanoparticle layers in the epoxy resin with an increase in the  $d$ -distance from 21.198 observed in Nanoclay. This demonstrated that Epoxy complex molecular networks were placed between nanoparticle layers [30].

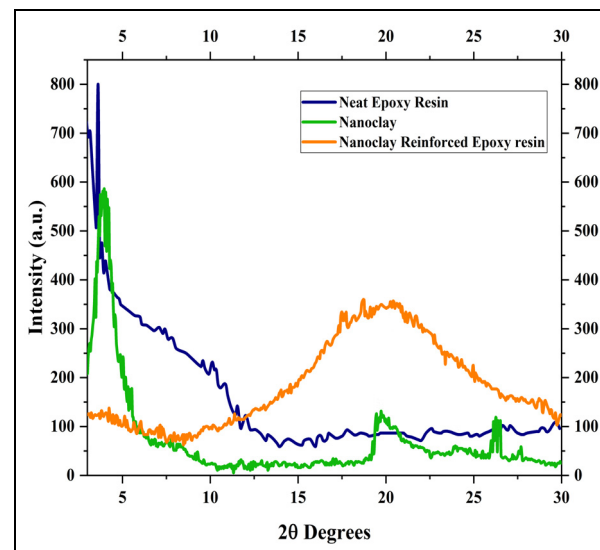


**Figure 3.** XRD patterns of the Epoxy and Epoxy toughened with Nanoclay.

The patterns obtained from XRD for epoxy resin and Graphene are represented in Figure 4. A shift of the peak of basal reflection from  $2\theta = 7.8^\circ$  to  $2\theta = 19.8^\circ$  is seen because of intercalation between the Graphene interlayer spacing and resin chains of Epoxy. A strong peak is observed at  $2\theta = 21.9^\circ$  which corresponds to 3.89 Å basal spacing. The peak observed indicates oxide structures of Graphene, which are absent in graphene-reinforced Epoxy due to the incidence of delamination

with epoxy resin. Another intercalation is observed at this peak of  $2\theta=21.9^\circ$  between the layers of Graphene and chains of epoxy resin [31-32].

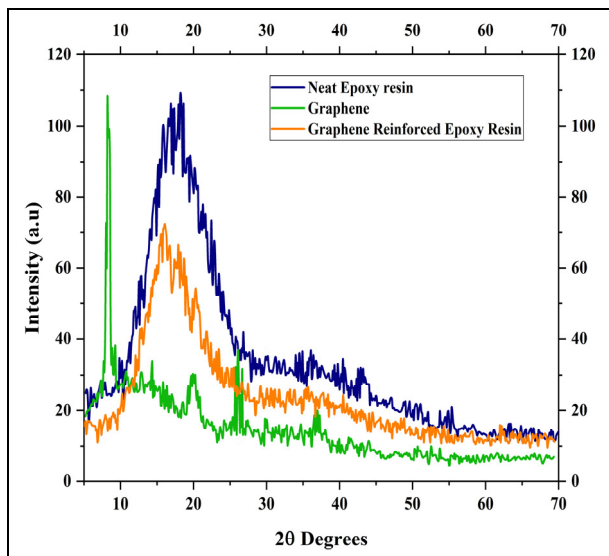


Figure 4. XRD patterns of the Epoxy and Epoxy toughened with Graphene.

## 2.2 Machining of Nano-PMCs - Thrust Force and Torque

The P.M.C. samples were subjected to drilling tests utilizing the Leadwell CNC machining center. The thrust force [ $T_f$ ] and Torque [ $T_m$ ] were measured using a SYSCON multi-component dynamometer. A charge amplifier amplified and processed the data to examine the force signals. The amplified signal was subjected to signal conditioning using specialist equipment and then connected to a computer system using a data acquisition card. The drill bits used were made of carbide materials and were of Brad and Spur types. The drill bits have sizes of 5, 6, 8, and 10 mm.

Figures 5 and 6 show the variations in thrust force during the drilling of Nanocomposites, comparing the cases with and without supports. The profile may be separated into three separate zones. Once the drill bit's chisel edge penetrates the top surface of the lamina, the thrust force in the first zone abruptly increases. In the second zone, the thrust force remains constant until the drill bit's chisel edge reaches the last layers of the lamina exit plane. In zone three, the drill bit experiences a fast drop in the forward force as it moves away from the bottom layer, eventually reaching zero. The thrust force remains constant throughout zone 2 until the drill bit's chisel edge breaks through the last layers of the lamina exit plane.

When the drill bit exits the lowest ply in zone 3, it experiences a rapid decline in thrust force until it reaches zero [33]. As the size of the cutting edges diminishes, the severity of the impact reduces, resulting in a reaming effect on the hole. Placing a supportive stack sheet underneath the laminates helps mitigate delamination caused by drilling, reducing deformations that lead to push-out delamination. Figure 6 shows the alteration in the thrust force profile while drilling the laminate with stack supports. Once the drill passes

through the final layer, the thrust force decreases briefly, followed by a sudden increase as the drill penetrates the uppermost layer of the Al stack support. The thrust force diminishes as it surpasses the 3 mm stack support [34].

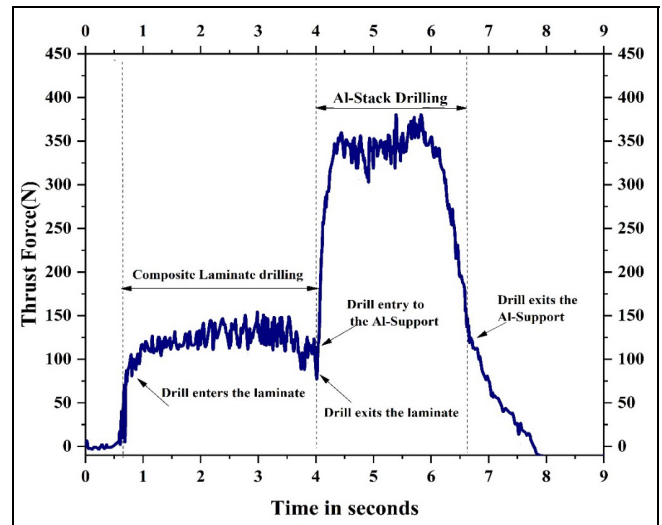


Figure 5. Variation of  $T_f$  in the Drilling of Nanocomposites without supports.

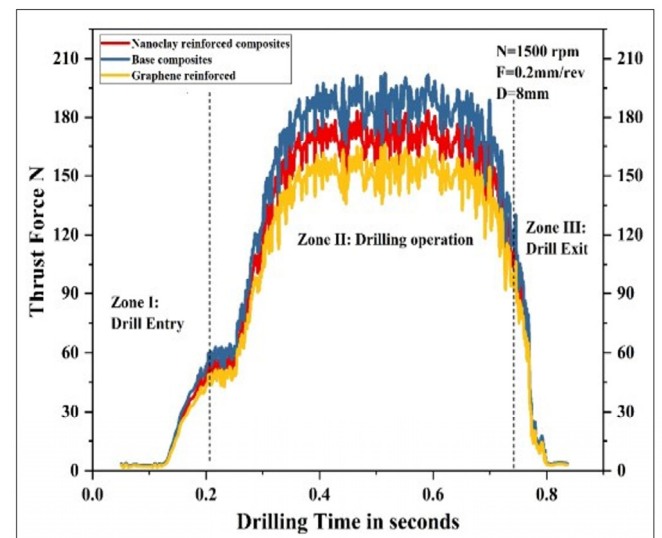


Figure 6. Variation of  $T_f$  in the Drilling of Nanocomposites with supports.

The torque variations during the drilling of Nano-composites display discrete phases, as seen in Figures 7 and 8. Within the zone of initial thrust force, there is a notable increase in torque magnitude. During the second phase, the torque signal exhibits an upward slope as the drill bit begins to cut, resulting in the softening of the Epoxy. At this stage, the frictional force generated by the contact between the tool and the composites becomes insignificant.

During the last phase, the torque values significantly reduce when the drill bit gets closer to the last layers and the depth drops. The decrease becomes more pronounced when smaller cutting edges are involved, resulting in a reaming impact on the hole [35–36]. The torque profile changes are similar to those observed in the thrust profile, as depicted in Figure 8, mainly when stacks support drilling. This insight into the torque

dynamics provides a comprehensive understanding of the drilling process for nanocomposites and underscores the impact of support mechanisms on torque variations during laminate drilling [37].

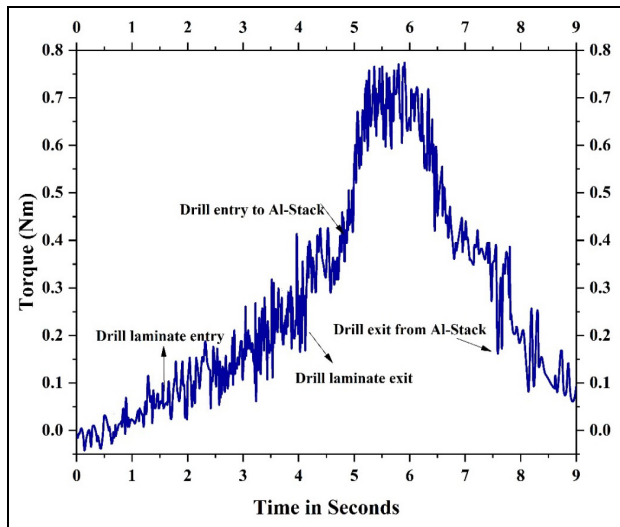


Figure 7. Variation of Torque in the Drilling of Nanocomposites with supports.

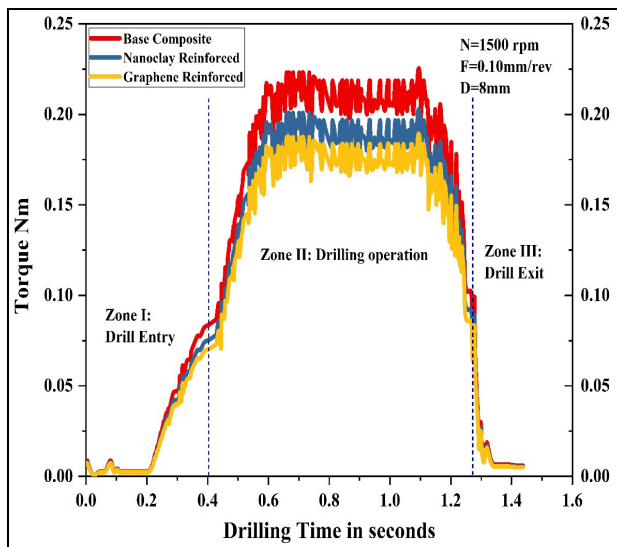


Figure 8. Variation of Torque in the Drilling of Nanocomposites without supports.

### 2.3 Experimental Design

All feasible combinations for a given set of elements are identified through a complete factorial design of tests. Only a limited group of options are chosen from all the possibilities to keep the number of tests manageable. The Taguchi method, also known as robust design of experiments (D.O.E.), outlines the essential tests necessary to fully understand all elements that affect performance. The governable factors influence the quality of drilled holes in composite laminates and their residual tensile strength.

Every traditional orthogonal array has a fixed number of design variables and levels. This investigation utilizes the L16 orthogonal array. We analyze each of the three independent variables at four different levels. The study design used an experimental approach with three components and four levels. We built the

design using the Taguchi L16 method, as shown in Table 2. Table 3 includes the comprehensive Design of Experiments (D.O.E.). For each experiment number in the table, we conducted five trials.

Without employing ANOVA, Taguchi proposes examining the S/N ratio using a theoretical method that involves charting the influences and graphically selecting the elements that seem to be relevant. This is a significant response to researching the drilling process's efficiency. To assess a design's efficacy, the influence of its parameters on the outcome must be measured. The word signal refers to a close-to-target predicted output. Noise is an unwanted element that measures output variation.

Table 2. Drilling Factors and Levels.

Factor	Level 1	Level 2	Level 3	Level 4
Speed (rpm)	1000	1500	2000	2500
Feed rate (mm/rev)	0.05	0.1	0.15	0.20
Drill tool diameter (mm)	5	6	8	10

Table 3. Taguchi L16 Design of Experiments

Experiment Number	Spindle Speed R.P.M.	Feed Rate mm/rev	Drill Tool Diameter mm
1	1000	0.05	5
2	1000	0.1	6
3	1000	0.15	8
4	1000	0.2	10
5	1500	0.05	6
6	1500	0.1	5
7	1500	0.15	10
8	1500	0.2	8
9	2000	0.05	8
10	2000	0.1	10
11	2000	0.15	5
12	2000	0.2	6
13	2500	0.05	10
14	2500	0.1	8
15	2500	0.15	6
16	2500	0.2	5

### 2.4 Assessment of Residual Tensile Strength

During drilling operations, a significant variation in thrust force and Torque was noted in various machining conditions, and this caused changes in damage around the hole, such as delamination, micro fractures, fiber pull out, and fuzzing of matrix, as well as variations in residual strength in the regions around the drilled holes [38]. The damage caused by drilling Fibre Reinforced Polymer laminates might damage the product's mechanical performance.

A Universal Testing Machine made by Instron was used to measure the residual strength of the drilled specimens. ASTM D3039 standards were used to cut the samples, and a schematic model is shown in Figure 9. The spindle speed and feed rate were maintained according to experimental number 9 under the support and without support conditions, as well as before and after tool wear conditions.

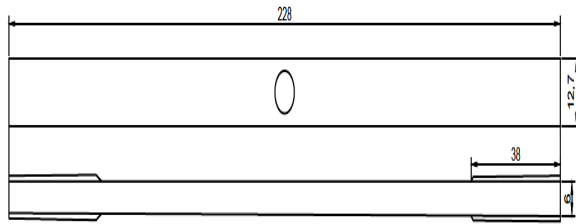


**Figure 9. Schematic representation of the residual tensile strength specimen**

## 2.5 Assessment of Tool wear

Many challenges arose during the machining process of P.M.C.s, including notable tool degradation, inferior surface quality on the finished components, and cracks and delamination in the underlying layers. We evaluated the hole's quality by considering its diameter, the  $D_f$  at the entrance and exit planes, and other flaws associated with surface damage. Identifying tool wear is challenging due to the complexity of drilling anisotropic composite materials. According to research, using a worn-out tool during drilling increases delamination and decreases structural integrity due to the elevated cutting force and vibration experienced during machining. Consequently, it is necessary to replace the worn-out tool at regular intervals throughout the machining operation [39]. In the present investigation, the tool wear assessment was carried out on specimens with support and without support for the case study mentioned as experiment number 9 in the experimental design table. Eighty holes were drilled on all three composites, and tool wear assessment and thrust force were carried out after drilling ten holes.

As a result, to prevent delamination of drilled components, it's critical to keep an eye on the drill bit's condition while machining composites. Drilling tests were carried out continuously for up to eighty holes with a single drill bit according to the experimental plan. The difference in the drill's land width before and after machining was used to calculate flank wear. The measurements were taken using a toolmaker's microscope, and the data were analyzed using the mean flank wear of the three replications. The tool wear, thrust force, and Torque were recorded for every tenth hole measured. The delamination factor and residual strength were assessed to know the effect of wear on the drilled holes.

## 3. RESULTS AND DISCUSSIONS

### 3.1 Delamination Factor Assessment

The research was conducted according to the Taguchi L16 experimental design, and the findings are reported in Table 4. The image-processing technology in MATLAB, Image J, and the Buckingham theorem methodology [40] have been used to determine the delamination factors. An average delamination factor was determined by considering five holes for each experiment number. The drilling of laminates with and without supports was performed under dry conditions.

The morphological and dimensional limitations have proved challenging due to the polymeric composites' material anisotropy. Delamination at the exit and

entrance planes, damage associated with generating and dissipation of heat, and geometrical defects were the leading causes of failures detected during the drilling. The interplay between the drill's cutting edge and the fiber's orientation might cause tool geometry damage, too. The geometry or drilled hole circularity is impacted by the principal axes conforming to the direction of the fibers since the fibers are considerably exposed to alternating phases of tensile and compressive loads before shearing. As discussed, two separate mechanisms create delamination at the workpiece's entrance or departure. The effect on the entry plane is minimal in the presence of the stack supports and considerably influences the delamination factor on the exit plane [41].

**Table 4. Experimental Results of Delamination Factor.**

Exp. No.	Entry Plane-Delamination Factor		
	Base Composite ( $F_d$ BC)	Nano Clay Reinforced ( $F_d$ NC)	Graphene Reinforced ( $F_d$ GR)
1	1.048	1.009	1.0084
2	1.130	1.091	1.05261
3	1.203	1.162	1.12048
4	1.265	1.222	1.17833
5	1.057	1.0211	1.0206
6	1.120	1.0824	1.04344
7	1.188	1.147	1.10652
8	1.143	1.104	1.06445
9	1.095	1.059	1.037
10	1.100	1.063	1.045
11	1.125	1.087	1.04807
12	1.155	1.116	1.076
13	1.015	1.012	1.0116
14	1.078	1.041	1.00411
15	1.117	1.079	1.04018
16	1.147	1.108	1.06877
$\sigma$	0.06509	0.05987	0.04771

The drill flute's upward axial stress on the cut layers causes peel-up delamination at interfaces proximal to the hole entry. This force induces a peeling action, causing the upper layers to separate from the uncut layers and resulting in delamination along the hole's border. As the drill gets closer to the bottom surface of the workpiece, there is a separation between layers at the hole exit, known as push-out delamination. When the thrust force surpasses a critical threshold, corresponding to the crack propagation at the layer interfaces, the drill's force bends the entire laminate region, initiating delamination [42]. It is noteworthy that push-out delamination is more severe and poses a more significant threat to structural integrity than peel-up delamination. Hence, the assessment of the delamination factor at the exit plane is significant. In the epoxy matrix, Nanoclay and Graphene particles act as stress transfer agents, causing plastic deformation in the base material and increasing the strength of the nanocomposite [43-44]. The amino groups in Nanoclay and the ability to divert cracks increased Epoxy's fracture toughness and interlaminar shear strength. Nanoclay regions will resist crack propagation, resulting in fracture winding. The epoxy matrix reinforced by Nanoclay becomes more durable due to a larger surface area [45].

Many studies have found that combining Epoxy and Graphene increases modulus and toughness. Fracture toughness and flexural modulus increased as filler content increased, indicating that Graphene significantly impacted Epoxy. Delamination may be efficiently controlled or avoided by reducing the feed rate as it approaches the exit and employing backup support plates to support and resist bending the composite laminate that causes delamination on the exit side [46]. Backup/support plates help decrease delamination, as shown in Table 5.

The function of the hole diameter is straightforward: according to the delamination factor's formula, the wider the size of the hole, the more significant the delamination area for a given delamination factor. As a result, laminates with bigger holes have a more seriously damaged surface at the same delamination factor [47]. The interaction of contact force between the drill bit and the drilled hole surface causes heat transfer-related damage.

**Table 5. Experimental Results of Delamination Factor with and without supports.**

Exp. No.	Exit Plane-Delamination Factor without support			Exit Plane-Delamination Factor with support		
	(F <sub>d</sub> BC)	(F <sub>d</sub> NC)	(F <sub>d</sub> GR)	(F <sub>d</sub> BC)	(F <sub>d</sub> NC)	(F <sub>d</sub> GR)
1	1.188	1.085	1.015	1.145	1.045	1.006
2	1.284	1.1741	1.097	1.237	1.131	1.078
3	1.367	1.249	1.168	1.317	1.203	1.125
4	1.438	1.314	1.228	1.386	1.266	1.183
5	1.201	1.097	1.026	1.157	1.057	1.021
6	1.273	1.163	1.088	1.227	1.121	1.068
7	1.35	1.234	1.153	1.303	1.191	1.113
8	1.299	1.187	1.116	1.254	1.146	1.072
9	1.187	1.085	1.055	1.146	1.048	1.019
10	1.251	1.143	1.069	1.207	1.104	1.044
11	1.279	1.169	1.093	1.235	1.129	1.055
12	1.313	1.263	1.122	1.268	1.159	1.083
13	1.154	1.054	1.033	1.113	1.017	1.001
14	1.225	1.126	1.047	1.182	1.080	1.015
15	1.269	1.168	1.084	1.224	1.119	1.051
16	1.304	1.192	1.114	1.258	1.150	1.080
$\sigma$	0.0717	0.0655	0.0544	0.0690	0.0631	0.0499

The evaluation of the delamination factor on the exit layer is significant concerning the entering layer. Inter-layer normal stress arises between the matrix and the fibers as the tool approaches the exit plane. Since all fibers have not been cut, delamination occurs in the interfacial area [48]. Intra-layer delamination with microfractures is caused by matrix fuzzing and matrix spalling when the feed rate increases. The interlaminar matrix shear strength rises with the addition of Nanoclay or Graphene, aiding the reduction of delamination [49].

### 3.2 Effect of Thrust Force [T<sub>r</sub>] and Torque [T<sub>m</sub>]

Thrust force [T<sub>r</sub>] and Torque [T<sub>m</sub>] generated during composite laminate drilling are affected by input parameters such as spindle speed (rpm), feed rate (mm/rev),

drill bit shape, tool wear caused by drilling number of holes, and drilling conditions. The rapid growth of drilling-induced delamination regions with increased feed rates and lower spindle speeds is evident. As the drill spindle rpm increases, so do the cutting pressures, and the severe heat accumulation in the machining area adds to fiber and matrix softening. Laminate Drilling for the cutting edges of tools becomes more challenging as the drilling length increases with a decrease in feed rate. More heat is generated and transferred to the laminate in the drilled hole region. Fiber breakage is often the primary reason, but at low rpm, fiber tearing out has been discovered to be the leading cause of higher delamination compared to mid-speed levels [50]. As demonstrated in Table 6, increasing spindle rpm causes a reduction in cutting forces. The reduction in thrust force [T<sub>r</sub>] and Torque [T<sub>m</sub>] at higher spindle rpm is the consequence of the epoxy matrix being less rigid owing to an increase in temperature, as well as the E-glass fibers having a low coefficient of heat conductivity [51]. The feed rate has a significant influence; as it increases, the thrust force also increases, and a combination of lower feed rates with higher spindle speeds enhances composite drilling by minimizing mechanical structural integrity loss. Simultaneously, reducing the feed rates might also result in the thermal deterioration of the epoxy matrix [52–53].

**Table 6. T<sub>r</sub> and T<sub>m</sub> on the exiting surface of composite materials.**

Exp. No.	T <sub>r</sub> BC (N)	T <sub>r</sub> N.C.R. (N)	T <sub>r</sub> Gr (N)	T <sub>m</sub> BC (Nm)	T <sub>m</sub> N.C.R. (Nm)	T <sub>m</sub> Gr (Nm)
1	151.61	131.10	121.92	0.262	0.233	0.220
2	179.46	155.20	144.34	0.338	0.301	0.284
3	196.4	169.85	157.96	0.503	0.448	0.423
4	228.78	197.85	184.00	0.721	0.642	0.606
5	136.22	117.80	109.55	0.250	0.222	0.210
6	156.96	135.74	126.24	0.353	0.314	0.296
7	180.45	156.05	145.13	0.467	0.416	0.393
8	208.76	180.53	167.89	0.604	0.538	0.508
9	129.49	111.98	104.14	0.213	0.190	0.179
10	144.49	124.96	116.21	0.236	0.210	0.198
11	161.32	139.51	129.74	0.448	0.399	0.377
12	189.21	163.63	152.18	0.554	0.493	0.465
13	114.77	99.25	92.30	0.251	0.224	0.211
14	132.30	114.41	106.40	0.298	0.265	0.250
15	152.6	131.97	122.73	0.439	0.391	0.369
16	172.6	149.26	138.82	0.463	0.412	0.389
$\sigma$	31.168	26.955	25.070	0.149	0.132	0.125

With the negative rake angle at a greater feed rate, glass fibers in laminates are pushed rather than sheared. Delamination occurs less often at greater feed rates, but inter-laminar fractures are detected near high-density locations [54]. The data shows that increasing the drill diameter causes more delamination damage when drilling composite materials. This phenomenon occurs because an increase in drill bit diameter expands the surface area of the drilled hole. Consequently, the drilling process on composite laminates increases the thrust force. The extent of drilling-induced delamination likewise increases as the thrust magnitude advances.

High feed rates, low spindle speeds, and large drill tool sizes significantly affect the variability in thrust force [55]. Figures 10 and 11 depict the relationship between thrust force, feed rate, and spindle speed for the base composite, Nano Clay reinforced composite, and Graphene reinforced composite. The support given during the drilling process for the laminate underneath the workpiece may help to resist the bending of the individual layers caused by the force applied during drilling. Initially, the support material fully touches the bottom of the workpiece, exerting a consistent upward force on its backside. During the drilling process, the laminate undergoes deformation. The support body exhibits much greater rigidity compared to the flexible, thin laminae and does not completely conform to deflection [56].

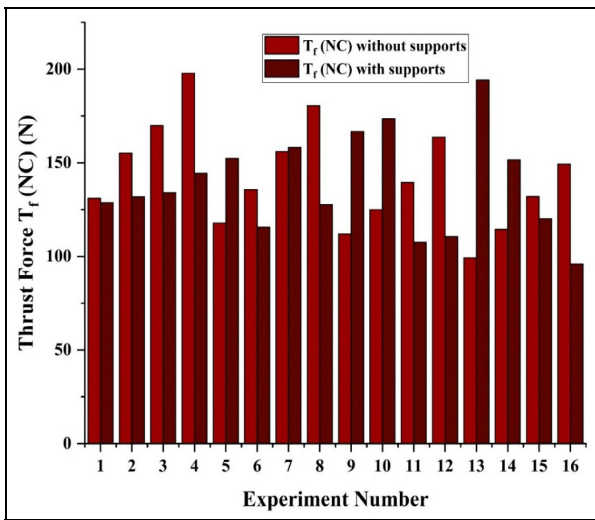


Figure 10. Comparison of  $T_r$  with and without supports in the B.C. reinforced with N.C.

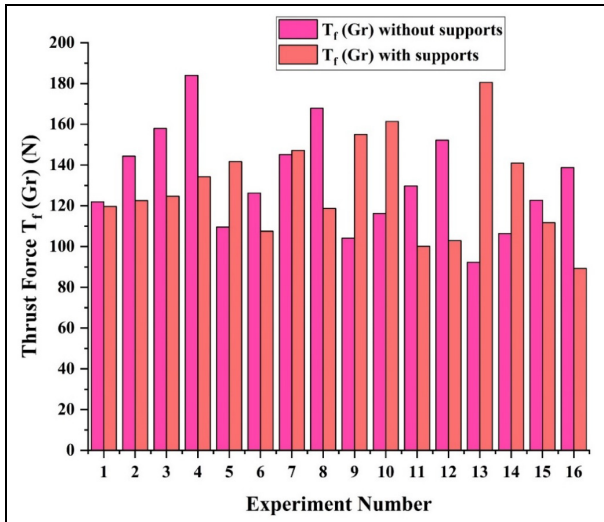


Figure 11. Comparison of  $T_r$  with and without supports in the B.C. reinforced with G.R.

The downward bending of the uncut laminate simultaneously generates an internal force that pulls the laminate from the edges of the circular fracture, causing the bottom side of the workpiece to make contact with the backup material at one location. More precisely, the central area at the bottom of the workpiece receives the distributed load. During the drilling process, the bent layers are responsive to both the force applied and the

support force. The figures above clearly demonstrate decreased Torque and thrust force under the supports. Figures 12, 13, and 14 specifically show that a decrease in the delamination factor beneath the support plates [57] accompanies the drop in thrust force. Cutting forces are beneficial for evaluating drill wear since they tend to rise as the tool wears. Cutting forces give a reliable evaluation of tool conditions throughout the tool wear zone. If the tool cannot handle the higher cutting forces, catastrophic tool failure will occur. As a result, measuring thrust force, a direct consequence of tool wear is the best way to evaluate tool life. The drilling of polymer requires real-time thrust force and torque monitoring.

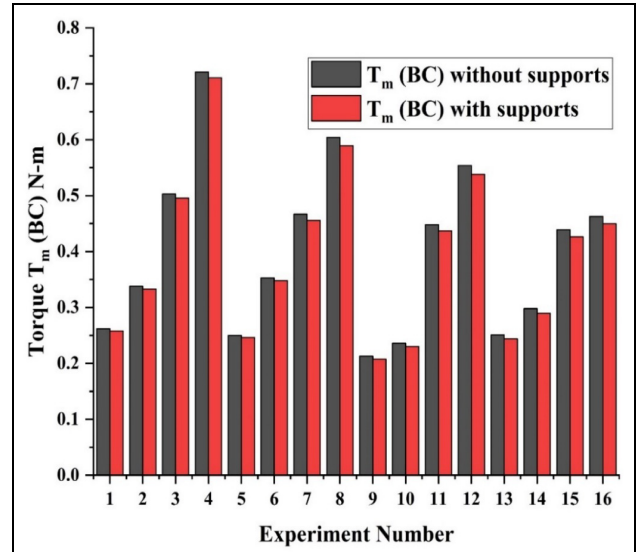


Figure 12. Comparison of Torque with and without supports in the B.C.

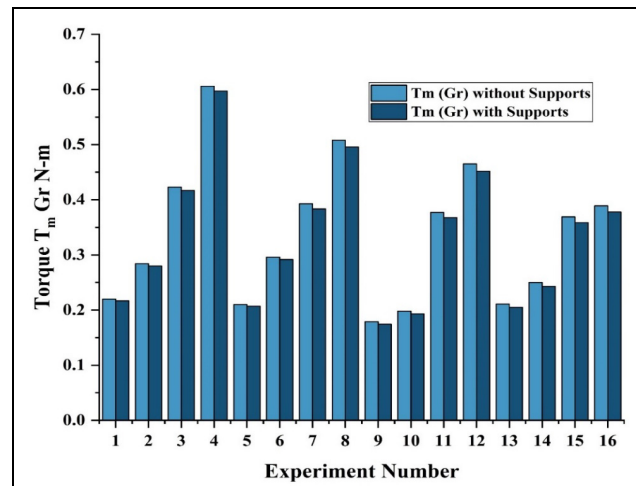


Figure 13. Comparison of Torque with and without supports in the B.C. reinforced with G.R.

The link between machining parameters, thrust force, Torque, and shear stress while drilling P.M.C.s has been the topic of many studies since they directly impact the machined hole's quality [58-59].

Due to the entwining of the final fibers in the drill, the thrust force decreases (perhaps due to friction-induced matrix softening), but the Torque rises. Due to the elevated temperatures caused by the greater heat generation linked to the low thermal conduction



coefficient and low transition temperature of plastics, increasing the spindle speed decreased thrust force and Torque [60].

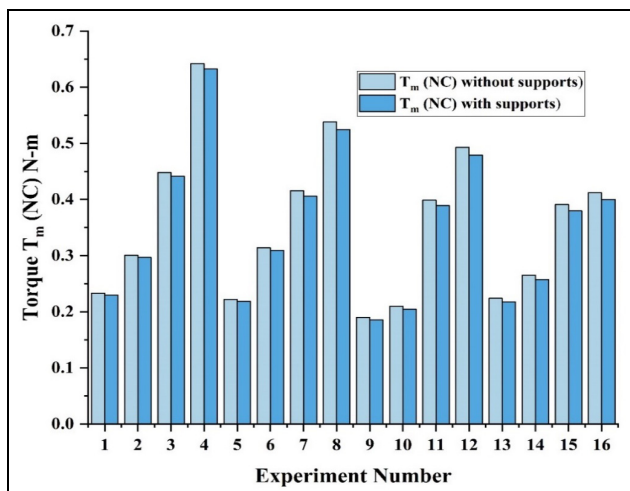


**Figure 14. Comparison of Torque with and without supports in the B.C. reinforced with N.C.**

With a larger shear area, thrust force and Torque for larger diameter tools increase. At higher spindle speeds and smaller feeds, the nanoclay and graphene reinforcements help to prevent delamination. The composite laminate strength falls when the drill bit cuts the last few layers of the laminate layers, causing push-out delamination and the creation of uncut fibers owing to fracture at the matrix-fiber interface [61]. Delamination is prevented since the interlaminar shear strength of nanoparticle-reinforced laminates is higher than the base composites. The activation energies for neat epoxy systems are lower than the unfilled nanoparticle epoxy systems, which can be attributed to the catalytic activity between Nanoclay/Graphene and Epoxy during the initial reaction stages leading to the exfoliation of the nanoparticles in the matrix system [62].

### 3.3 Tool Wear Effect on Thrust Force and Delamination Factor

The increase in the cross-sectional area of the chip causes the drill diameter to be 8 mm and the feed rate to be 0.2 mm/rev, influencing the chip's ability to break. Nevertheless, the impact of a spindle speed of 2000 rpm seems to be diminished, and throughout the drilling operation, smaller pieces are favoured. The present study conducted a tool wear analysis for the given machining process, considering the impact of the metal stack support and its absence. Disposal of chips, fluctuations in machining forces, the influence of temperature on a tool, and wear are all obstacles encountered while drilling a stack of composite material and metal. E-Glass/Epoxy composite chips exhibit a continuous form while the feed rates are low but transform into fine particles resembling dust when the feed rates are increased. According to reference [63], the Aluminum chips will have a continuous form when the spindle speed is high and the feed rate is low. The presence of continuous and high-temperature chips in the E-Glass/Epoxy composite adversely affects the quality of the holes when Aluminium is layered at the

bottom. When drilling ductile Aluminium and very abrasive E-Glass fiber, it is important to balance the cutting tool and process parameters. Our study indicates that the literature on composite material-metal stacks is scarce. Multiple sources confirm that the material often employed in aeroplane construction is generally E-glass-fiber-reinforced plastic. Composite materials are often employed on a stack's upper and lower parts when constructed using Aluminium or titanium [64].

Figure 15 depicts a standard variation in drilling thrust force, whereas Figure 16 illustrates the impact of tool wear on thrust force. The graphs show the relationship between the force the drill exerts at various stages, including when it enters the material, fully engages with the tool and exits the workpiece's final layers. The thrust force initially rises with two distinct discontinuities (arrows a and b), regardless of the number of drilled holes (H.N.). Specific geometrical features of the tool point cause these discontinuities. Point 'b' indicates the entry of the primary cutting edges into the workpiece, coinciding with a sudden change in the profile shape, as discussed in earlier sections.

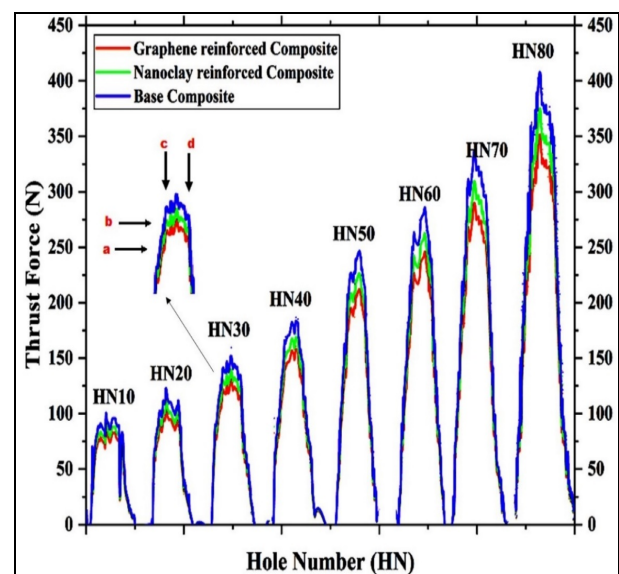


**Figure 15. Variation of  $T_f$  against the H.N.**

The second stage starts at point "c," where the leading cutting edges are fully engaged. This stage is different because the force signal changes, the material composition changes, and the fibers' orientation changes constantly, affecting the cutting direction. During the third step, when the chisel edge reaches point 'd' on the rear surface of the laminate, the thrust force decreases, and the cutting edges at the front no longer make contact with the workpiece. The force decreases to zero once the leading cutting edges move away from the hole. At this point, reaming begins, and only the leading cutting edges come into contact with the hole wall [65]. The study demonstrated a positive correlation between the number of drilled holes and tool wear. The entrance and exit areas of the drilled composite exhibit two contrasting tendencies. During the first drilling process, the delamination factor is enhanced when the drill bit's cutting edges come into contact with the composite material. The peeling force generated by the inclined surface of the drill then causes the layers of the material

to separate from each other. As the edge deteriorates, the force diminishes due to the reduction in sharpness.

Consequently, the thrust force rises, and the peel force reduces, leading to a reduction in peel-up delamination and an increase in push-out delamination processes. When the cutting edges of the drill bit come into contact with the material, the slope of the drill causes the layers to separate from one another due to a peeling force. When the edge starts to deteriorate due to a loss in sharpness, the force diminishes. As the thrust force increases and the peel force decreases, there is a drop in peel-up (which causes delamination at the entrance of a hole) and an increase in push-out (which causes delamination at the exit) processes [66].

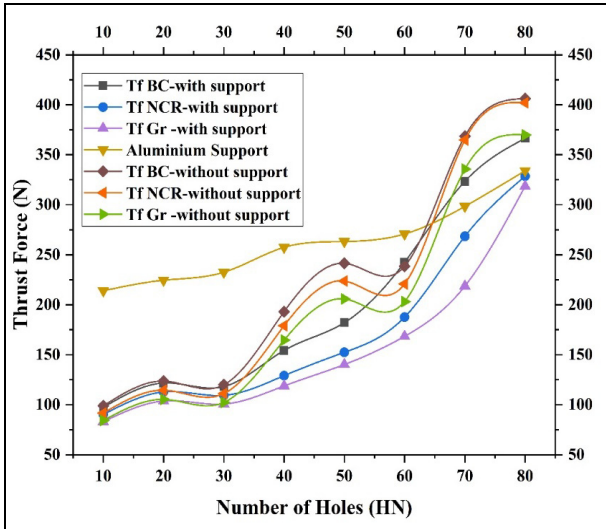


Figure 16. Variation of Thrust force with tool wear.

Several researchers have made a similar finding. During drilling, due to the difference in the resin and fiber elastic stresses and the cutting-edge radius of the carbide tip drill, the delamination factor of E-Glass/Epoxy composites was lowered from 10 to 30 holes, according to measurements as shown in Figure 17. The inclination to reduce hole diameter increases friction between the drill and the hole surface when drilling Al from 40-60 holes. The delamination factor rises because of difficulties evacuating Al chips through the drilled holes. The wear area can be identified as the initial wear region where we achieve effective machining of the composites. The current investigation is in the region of 10-30 holes. We witnessed a region of fast wear, with 40-60 holes that may require re-sharpening of the tool, and the final region of wear, around 70-80 holes, which suggests a tool change or damage. These regions vary with the number of holes drilled, specimen material, geometry, and tool material. These regions aid in delamination factor optimization and improve the circularity ratio of the drilled holes in the P.M.C.s [67]. Stack support has minimal influence on the entrance plane. On the exit plane, the delamination factor increases for the given condition since the thrust forces increase with and without supports. The behaviour is like analyzing the circularity ratio for the drilled holes. The  $T_f$  increases gradually up to thirty holes during the Drilling of E-glass/Epoxy composites, as it falls in the effective machining region,

aiding the formation of a stable cutting-edge radius. Figure 17 shows the effect of tool wear on the  $D_f$  on the entry and exit plane. The circularity ratio decreases on the entry plane in the initial wear region, and the circularity ratio improves from 40-80 holes in the secondary wear region.

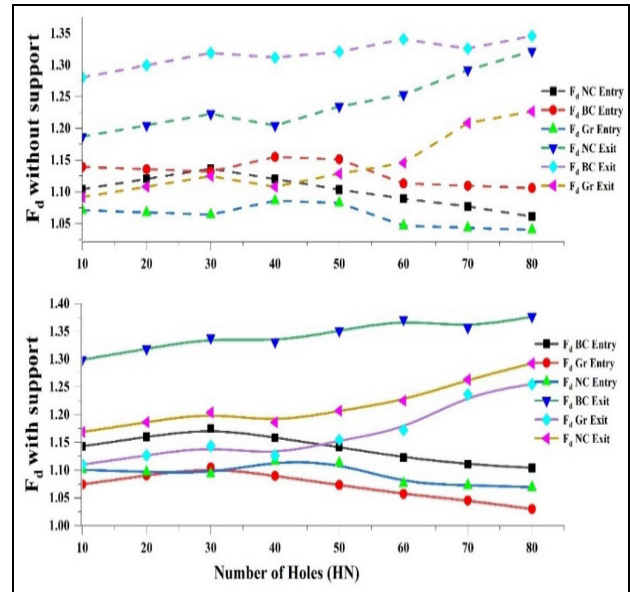


Figure 17. Delamination factor on entry and exit plane post tool wear.

However, the contrast is witnessed on the exit plane with or without supports, and the circularity ratio decreases in the initial region the variation is minimal, and around 40-50 holes and as the tool enters the final wear zone, which decreases the circularity of the holes as shown in Figure 18.

This area might be ascribed to normal wear since it has a steady cutting force between thirty and sixty holes and falls in the region of resharping the tool. This range is perfect for drilling E-glass, Epoxy, and Al stacks, as shown in Figure 19. Beyond 60, the thrust forces progressively increase, probably owing to decreased cutting-edge sharpness.

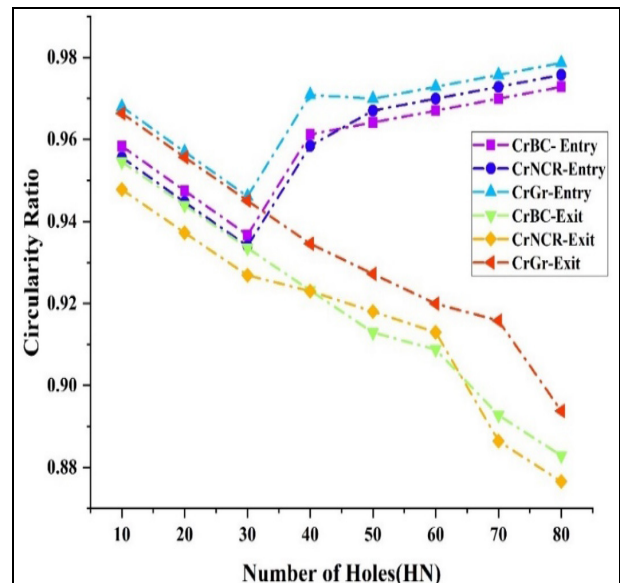
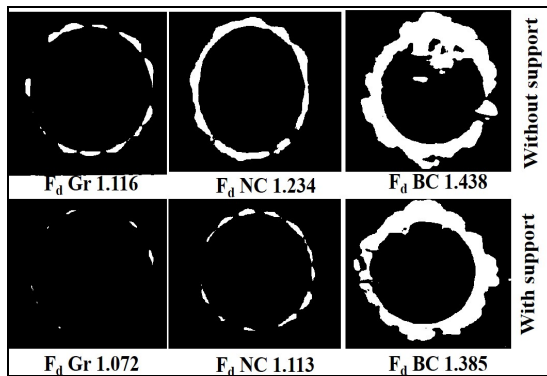


Figure 18. Circularity ratio on entry and exit plane post tool wear.



**Figure 19. Effect of Al stack support on exit plane delamination factor.**

When tool wear increases, the material removal technique changes with reduced tool performance due to fiber buckling [68]. These buckled fibers increase the tool wear and damage the drilled hole surface. The surface finish in the Al metal stack was not affected much, and it was in the range of 1-1.5 $\mu$ m), and only the composite material suffered the change in the surface finish. Compared to moderate speed, it is established that fiber fracture is the dominant factor at high speeds, and fiber pull-out is the dominant component at low speeds for enhanced delamination.

As shown in Figures 20 and 21, the SEM micrographs indicate the damage of tool wear on the hole's drilled surface. The variation of the delamination factor has been shown in Figure 22 through processed images of the drilled holes using MATLAB. The increased number of holes results in higher delamination on the exit plane.

The graphene-reinforced composites had less damage than the base composite, and the nanoclay composites also had more secondary damage under post-tool wear after 80 holes. The stack supports minimized the effects of exit delamination, but after 80 holes, the tool had to be replaced. The toughening of the epoxy resin prevents a reduction in tensile strength. Because nanoparticles of Graphene and Nanoclay integrate better into the epoxy resin microstructure when they reach almost molecular dimensions, and they restrict matrix deformation [69].

They may impact deformation processes in the polymer on the micro- or even nanoscale, depending on how strong their interactions are with the epoxy resin matrix. Nanoparticles encourage the prevention of many subcritical microcracks, delaying the coalescence of these microcracks into critical fractures [70]. Further the nanoparticles branch the microcracks reducing the crack propagation.

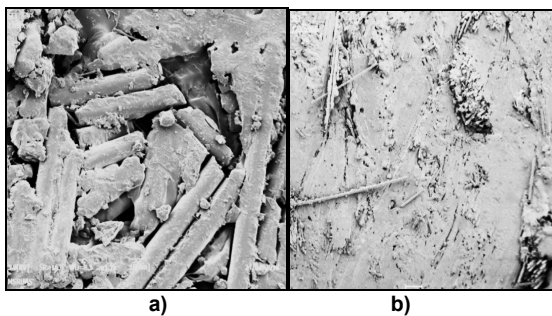


**Figure 20. Drilled hole surface post tool wear without supports a) NC and b) GR reinforced.**



**Figure 21. Drilled hole surface of the B.C. without support post tool wear.**

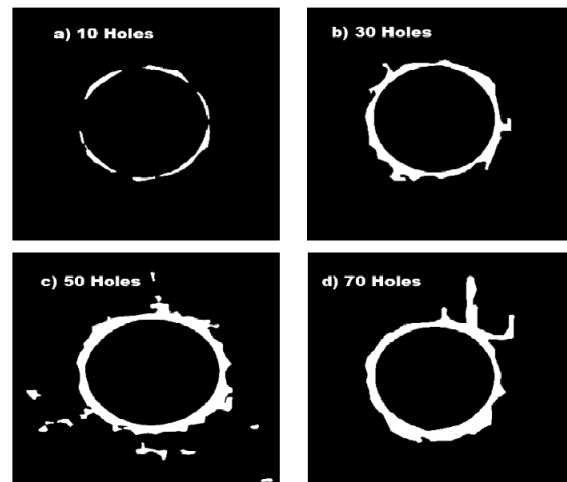


**Figure 22. Tool wear effect on delamination factor.**

### 3.4 Delamination Factor Effect on Residual Strength

The delamination region is just a tiny part of the laminate's width whenever the delamination factor is low. As a result, the stress distribution in the damaged region is unaffected by the free edge. The delamination factor may be employed to explain how delamination affects strength. The influence from free edges, on the other hand, increases as the delamination factor increases. Larger hole sizes indicate more effect from the free edges, further reducing strength [71]. Another expert examination found that laminates with moulded holes had a tensile strength of 20–30% greater than laminates with drilled holes. It is most likely the result of drilling-related flaws other than delamination, and a moulded hole is supposed to be able to prevent all of these flaws. The decrease in the tensile strength is around 5-6% for drilled holes without the support and about 4-5%, as shown in Table 7 and Figure 23. The loss of tensile strength is around 8-12% under the tool wear conditions. The loss of tensile strength due to delamination is critical. The decrease due to stiffness loss is small compared to the reduction driven by early failure. Because of its fiber orientation, the unidirectional ply with 0° is a crucial influence on the tensile strength of laminates.

The outermost 0° plies should be a key influence for strength decrease since drilling caused delamination primarily at the outer 0/45° contact. Compared to unidirectional fibers, woven fibers can reduce tensile strength loss [72]. Moreover, the proportion of fiber and void around the hole differs in laminates with drilled and moulded holes. Consequently, this work does not include developing a new numerical model designed explicitly for assessing laminates with moulded holes. Nonetheless, delamination alone causes enough damage to the laminates to significantly impair tensile strength. The loss of strength is primarily due to the early failure of the outer plies caused by the damaged interface's inability to transmit stress from plies to plies. The primary factor is the size of the delamination region or the delamination factor [73].

Smaller effect parameters, such as laminate geometries, toughening agents of resin, and hole width, might also influence residual strength. Better stress transfer between the fiber and the resin decreases the local stress concentrations around the drilled holes, improves the toughness and damage tolerance of the matrix, and improves energy dissipation under drilling. These qualities have reduced residual strength within 12% of its base strength under various machining conditions. The reduction of flaws is essential for toughening fragile epoxy matrices and increasing residual tensile stresses [74].

More crucially, delamination may have a far more considerable influence on long-term performance than static strength.

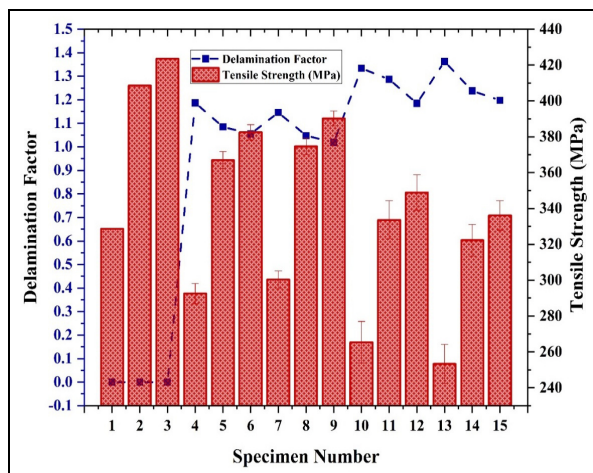


Figure 23. Comparison of residual Tensile strength for various specimens.

As a result, additional study into the impact of delamination on fatigue is needed. High aspect ratio fillers of Nanoclay and Graphene for use in Epoxy were proposed in this study to enhance various qualities to achieve a higher rigidity than the matrix to increase stiffness and boost structural rigidity. Although the surface activity of the Nanoclay and Graphene is unclear, they may engage in the epoxy curing process, resulting in distinct epoxy network architectures. This might play a role in the toughening effect shown in this study. The S.E.M. images in Figures 24-26 represent the internal fracture post the tensile test. It has been claimed that crack redirection mechanisms at particle barriers in

an epoxy resin matrix play a significant role in toughening [75]. It is considered that a crack may have deviated at a barrier and that bending and twisting forces it to migrate off its original propagation plane.

Table 7. Comparison of residual tensile strength under different conditions

Specimen Name	DF	Tensile Strength (MPa) [ASTM 3039]	%Change in Tensile Strength
Base Composite-Undrilled	-	328.60	-
Nano clay reinforced-Undrilled	-	408.60	-
Graphene reinforced-Undrilled	-	423.50	-
Base Composite-drilled without support	1.187	292.51	↓ 5.651 %
Nano clay reinforced-drilled without support	1.085	366.92	↓ 4.823 %
Graphene reinforced-without support	1.055	382.49	↓ 4.276 %
Base Composite-with support	1.14605	300.27	↓ 4.963 %
Nano clay reinforced-with support	1.04757	374.63	↓ 4.643 %
Graphene reinforced-with support	1.0186	390.19	↓ 4.177 %
Base Composite-Undrilled-Post tool wear without support	1.334	265.40	↓ 11.634 %
Nano clay reinforced-Post tool wear without support	1.287	333.63	↓ 10.665 %
Graphene reinforced-Post tool wear without support	1.185	348.89	↓ 9.865 %
Base Composite-Undrilled-Post tool wear with support	1.363	253.30	↓ 10.885 %
Nano clay reinforced-Post tool wear with support	1.238	322.29	↓ 8.814 %
Graphene reinforced-Post tool wear with support	1.198	336.08	↓ 8.256 %

When a crack bends or twists, the stress state changes from mode I to mixed mode. The pushing force required to propagate a fracture in mixed mode circumstances is more prominent than in mode I, resulting in a higher mechanical behaviour of the material. If the fracture pursues a 3D trajectory, the bending and twisting continue at succeeding particles. In this process holds, an improvement in the overall fracture toughness of an E-Glass/nanoparticle

toughened Epoxy composite may be predicted. Deflection processes enhance the fracture surface area compared to the fracture surface area created by an un-deflected crack.

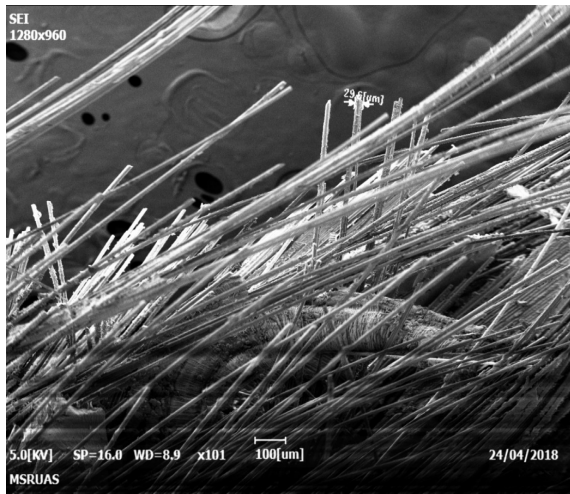


Figure 24. SEM image of B.C. drilled hole subjected to tensile test after 30 holes.

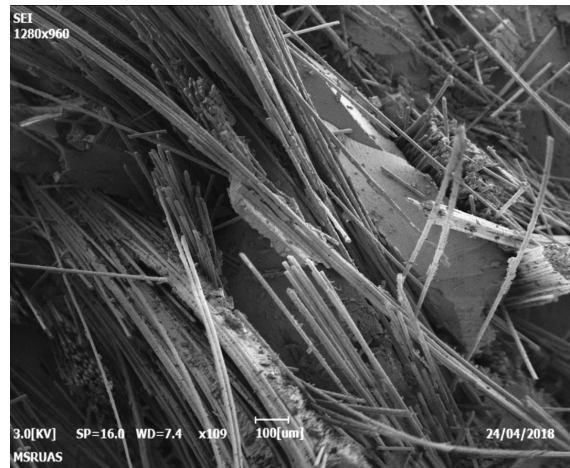


Figure 25. SEM image of N.C. reinforced composite drilled hole subjected to tensile test after 50 holes.

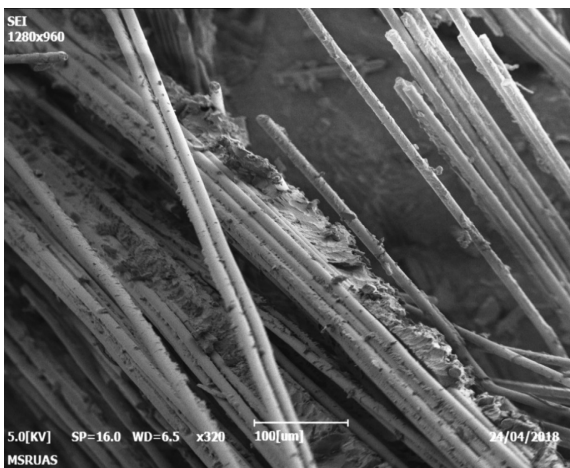


Figure 26. SEM image of G.R. reinforced composite drilled hole subjected to the tensile test after 70 holes.

#### 4. CONCLUSIONS

This research highlights a comprehensive grasp of the many factors involved in delamination mechanisms, the

consequences of tool wear, and residual tensile strength in composite materials during drilling procedures. Through the data synthesis, a clear and logical explanation develops, outlining essential insights relevant to selecting materials, optimizing processes, and improving structural integrity.

Firstly, using a Handlay process, augmented by E-Glass fibers and an epoxy resin matrix fortified with nanoparticles, exemplifies a strategic approach toward enhancing material properties. Sonication facilitated nanoparticle dispersion, which is crucial for reinforcing the matrix effectively. This meticulous methodology laid the foundation for subsequent investigations.

The XRD and FTIR tests provided clear evidence of including Nanoclay and Graphene in the epoxy matrix, confirming the effective integration of agents that enhance toughness. These reinforcements significantly reduced delamination, as shown by a noticeable drop in the delamination factor, especially in Graphene-reinforced composites.

In addition, support plates, while effectively reducing damage to the exit plane, highlighted the ongoing difficulty of preserving the structure's mechanical integrity during drilling activities. Although they successfully reduced delamination, their effectiveness was restricted to addressing laminate bending rather than providing complete mechanical support.

The intricate interplay between drilling parameters, composite anisotropy, and stress concentration phenomena is critical to structural integrity. Elevated stress concentrations around hole peripheries precipitated mechanical property degradation, underscoring the imperative of optimizing drilling parameters to mitigate such deleterious effects.

The influence of cutting conditions on composite damage was unequivocal, with higher spindle speeds and feed rates exacerbating damage propensity. Notably, thrust force escalation engendered a concomitant increase in delamination, elucidating the symbiotic relationship between these phenomena.

Amidst the myriad of challenges posed by drilling operations, the optimization of residual tensile strength emerged as a tangible avenue for structural enhancement. Manipulating feed rates and employing toughened polymer matrix composites (P.M.C.s) offer promising avenues for ameliorating residual tensile strength, thereby fortifying structural robustness.

This study underscores the intricate nexus between material composition, process parameters, and structural integrity within composite materials subjected to drilling operations. By elucidating key findings and their implications, this research catalyzes advancements in composite manufacturing, paving the path towards more resilient and durable structural components.

Future research can focus on adapting high-shear mixing to optimize nanoparticle dispersion in composite materials for matrix reinforcement. Incorporating nano rubber may improve toughness and delamination resistance. Adaptive drilling using real-time sensor data might reduce stress and increase structural integrity to improve composite performance suited for aerospace and automotive applications.

## REFERENCES

- [1] G.B. Veeresh Kumar, R Mageshvar, R Rejath, S Karthik, R Pramod, C S P Rao.: Characterization of glass fiber bituminous coal tar reinforced Polymer Matrix Composites for high-performance applications, *Composites Part B: Engineering*, Volume 175, 2019.
- [2] I. Suyambulingam, S. Mavinkere Rangappa, S. Siengchin.: *Advanced Materials and Technologies for Engineering Applications*, Applied Science and Engineering Progress, Vol. 16, No. 3 (Special Issue), 2023.
- [3] H. Hocheng, C.C Tsao.: Comprehensive analysis of delamination in drilling of composite materials with various drill bits, *Journal of Materials Processing Technology*, Volume 140, Issues 1–3, Pages 335-339, 2003.
- [4] J. Xu, V. Kolesnyk, C. Li, B. Lysenko, J. Peterka, M. Kumar Gupta.: A critical review addressing conventional twist drilling mechanisms and quality of CFRP/Ti stacks, *Journal of Materials Research and Technology*, Volume 24, Pages 6614-6651, 2023.
- [5] A. Sudam Shinde, I. Siva, Y. Munde, M. Thariq Hameed Sultan, Lee Seng Hua, Farah Syazwani Shahar.: Numerical modelling of drilling of fiber reinforced polymer matrix composite: a review, *Journal of Materials Research and Technology*, Volume 20, pp. 3561-3578, 2022.
- [6] R. Piquet, B. Ferret, F. Lachaud, P. Swider, Experimental Analysis of Drilling Damage in Thin Carbon/Epoxy Plate Using Special Drills, *Composites: Part A*, 31, pp.1107–1115, 2000.
- [7] Hossein Heidary, Mehdi Ahmadi, Abdolreza Rahimi, and Giangiacomo Minak.: Wavelet-based acoustic emission characterization of residual strength of drilled composite materials, *Journal of Composite Materials*, Vol.47(23), pp. 2897–2908, 2013.
- [8] Sathish Kumar Palaniappan, Manoj Kumar Singh, Sanjay Mavinkere Rangappa and Suchart Siengchin.: Eco-friendly Biocomposites: A Step Towards Achieving Sustainable Development Goals, *Applied Science and Engineering Progress*, Vol. 17, No. 4 (Special Issue), 7373, 2024.
- [9] J P.E. Faria, R.F. Campos, A.M. Abrão, G.C.D. Godoy and J.P. Davim, Thrust Force and wear Assessment When Drilling Glass Fiber-Reinforced Polymeric Composite, *Journal of Composite Materials*, Vol. 42: 1401, 2008.
- [10] Haonan Ma, Zhigang Dong, Zhongwang Wang, Feng Yang, Renke Kang, Yan Bao, Tool wear in cutting carbon fiber reinforced polymer/ceramic matrix composites: A review, *Composite Structures*, Vol. 337, 2024.
- [11] A.M. Abrão, P.E. Faria, J.C. Campos Rubio, P. Reis, J. Paulo Davim.: Drilling of fiber reinforced plastics: A review, *Journal of Materials Processing Technology*, Vol.186, pp.1–7, 2007.
- [12] Jae Hoon Ahn, Gyuho Kim, Byung-Kwon Min.: Exit delamination at the material interface in drilling of CFRP/metal stack, *Journal of Manufacturing Processes*, Vol.85, pp. 227-235, 2023.
- [13] Sbilir O, Ghassemieh E.: Three-dimensional numerical modelling of drilling of carbon fiber-reinforced plastic composites. *Journal of Composite Materials*. Vol.48(10), pp.1209-1219, 2014.
- [14] Goh Kai Ze, A. Pramanik, A.K. Basak, C. Prakash, S. Shankar, N. Radhika.: Challenges associated with drilling of carbon fiber reinforced polymer (CFRP) composites-A review, *Composites Part C*, Vol. 11, 2023.
- [15] Praveenkumara Jagadeesh, Sanjay Mavinkere Rangappa, Indran Suyambulingam, Suchart Siengchin, Madhu Puttegowda, Joseph Selvi Binoj, Sergey Gorbatyuk, Anish Khan, Mrityunjay Doddamani, Vincenzo Fiore, Marta María Moure Cuadrado.: Drilling characteristics and properties analysis of fiber reinforced polymer composites: A comprehensive review, *Heliyon*, Vol. 9, Issue 3, 2023.
- [16] Basavarajappa S, Venkatesh A, Gaitonde VN, Karnik SR.: Experimental Investigations on Some Aspects of Machinability in Drilling of Glass Epoxy Polymer Composites. *Journal of Thermoplastic Composite Materials*. Vol. 25(3), pp. 363-387, 2012.
- [17] Pramod, R., Basavarajappa, S. and Davim, J. Paulo.: 7. A review on investigations in drilling of fiber reinforced plastics. *Machinability of Fibre-Reinforced Plastics*, edited by J. Paulo Davim, Berlin, München, Boston: De Gruyter, pp. 179-194, 2015.
- [18] S. Kumar, S. R. Chauhan, P. K. Rakesh, I. Singh & J. P. Davim Drilling of Glass Fiber/Vinyl Ester Composites with Fillers, *Materials and Manufacturing Processes*, Vol.27:3, pp.314-319, 2012.
- [19] Arun K, Kumar DS, Murugesh M. Effect of TiO<sub>2</sub> and ZnS fillers on the bearing strength of gfrp composites. *Journal of Reinforced Plastics and Composites*, Vol.31(16), pp.1088-1096, 2012.
- [20] Jajam, K.C. Rahman, M.M. Hosur, M.V.Tippur, H.V.: Fracture behaviour of epoxy nanocomposites modified with polyol diluent and amino-functionalized multi-walled carbon nanotubes: A loading rate study, *Composites Part A: Applied Science and Manufacturing*, Vol. 59, pp. 57–69, April 2014.
- [21] Praveen D, Shashi Kumar M E, Pramod R.: Dielectric studies of Graphene and Glass Fiber reinforced composites, *I.O.P. Conf. Series: Materials Science and Engineering*, Vol.310, 2018.
- [22] N Raghavendra, H N Narasimha Murthy, K R Vishnu Mahesh, M Mylarappa, K P Ashik, D M K Siddeswara, M Krishna.: Effect of Nanoclays on the performance of Mechanical, Thermal and Flammability of Vinylester based nanocomposites,

- Materials Today: Proceedings*, Vol. 4, pp.12109–12117, 2017.
- [23] Ali Riza Motorcu, Ergün Ekici, Evaluation and Multi-Criteria Optimization of Surface Roughness, Deviation From Dimensional Accuracy and Roundness Error in Drilling CFRP/Ti6Al4 Stacks, *FME Transactions*, Vol. 50, pp.441-460, 2022.
- [24] Sridharan, V., Raja, T. & Muthukrishnan, N.: Study of the Effect of Matrix, Fibre Treatment and Graphene on Delamination by Drilling Jute/Epoxy Nanohybrid Composite. *Arab J Sci Eng*, Vol.41, pp.1883–1894, 2016.
- [25] Kinjal J. Shah, Atindra D. Shukla, Dinesh O. Shah, Toyoko Imae.: Effect of organic modifiers on dispersion of organoclay in polymer nanocomposites to improve mechanical properties, *Polymer*, Vol. 97, pp.525-532, 2016.
- [26] U.A. Khashaba.: Analysis of surface roughness, temperature, short aging, and residual notched and bearing strengths in supported drilling of thin GFRP composites, *Alexandria Engineering Journal*, Vol.86, pp.157-173, 2024.
- [27] Jianfeng Wang, Xiuxiu Jin, Chunhai Li, Wanjie Wang, Hong Wu, Shaoyun Guo.: Graphene and graphene derivatives toughening polymers: Toward high toughness and strength, *Chemical Engineering Journal*, Vol. 370, pp.831-854, 2019
- [28] Dave Kim, Aaron Bea, Kiweon Kang and Sang-Young Kim.: Hole quality assessment of drilled CFRP and CFRP-Ti stacks holes using polycrystalline diamond (P.C.D.) tools, *Carbon Letters*, Vol. 23, pp.1-8, 2017.
- [29] Zitoune R, Krishnaraj V, Collombet F.: Study of Drilling of composite material and Aluminium stack. *Compos Struct*, 92, 1246, 2010.
- [30] Jia Ge, Ming Luo, Dinghua Zhang, Giuseppe Catalanotti, Brian G. Falzon, John McClelland, Colm Higgins, Yan Jin, Dan Sun.: Temperature field evolution and thermal-mechanical interaction induced damage in drilling of thermoplastic CF/PEKK – A comparative study with thermoset C.F./epoxy, *Journal of Manufacturing Processes*, Vol. 88, pp.167-183, 2023.
- [31] R.A. Kishore, R. Tiwari, A. Dvivedi, I. Singh.: Taguchi analysis of the residual tensile strength after drilling in glass fiber reinforced epoxy composites, *Materials and Design*, Vol.30, pp.2186–2190, 2009.
- [32] Yu Bai, Zhen-yuan Jia, Rao Fu, Jia-xuan Hao, Fu-ji Wang.: Mechanical model for predicting thrust force with tool wear effects in drilling of unidirectional CFRP, *Composite Structures*, Vol.262, 2021.
- [33] Jinyang Xu, Norbert Geier, Jiaxin Shen, Vijayan Krishnaraj, S. Samsudeensadham.: A review on CFRP drilling: fundamental mechanisms, damage issues, and approaches toward high-quality drilling, *Journal of Materials Research and Technology*, Vol.24, pp.9677-9707, 2023.
- [34] De Fu Liu, Yong Jun Tang, W.L. Cong.: A review of mechanical drilling for composite laminates, *Composite Structures*, Vol.94, Issue 4, pp.1265-1279, 2012
- [35] Arun G K, Nikhil Sreenivas, Kesari Brahma Reddy, K Sai Krishna Reddy, Shashi Kumar M E, Pramod R.: Investigation on Mechanical Properties of Graphene Oxide reinforced GFRP, *I.O.P. Conf. Series: Materials Science and Engineering*, Vol.310, 2018
- [36] N Raghavendra, H N Narasimha Murthy, K R Vishnu Mahesh, M Mylarappa, K P Ashik, D M K Siddeswara, M Krishna.: Effect of Nanoclays on the performance of Mechanical, Thermal and Flammability of Vinylester based nanocomposites, *Materials Today: Proceedings*, Vol.4, pp.12109–12117, 2017.
- [37] Yazik, M. H. M., Sultan, M. T. H., Shah, A. U. M., Jawaid, M., & Mazlan, N. , Effect of nanoclay content on the thermal, mechanical and shape memory properties of epoxy nanocomposites. *Polymer Bulletin*, Vol.77(11), pp.5913-5931, 2019.
- [38] Xu, J., Li, C., Chen, M., Mansori, M., & Ren, F. (2019). an investigation of drilling high-strength cfrp composites using specialized drills. *The International Journal of Advanced Manufacturing Technology*, Vol.103(9-12), pp.3425-3442.
- [39] Anurag Thakur, Amrinder Pal Singh and Manu Sharma.: Mechanics of delamination-free drilling in polymer matrix composite laminates: A review, *Proc IMechE Part C:J Mechanical Engineering Science*, Vol. 235(1), pp.136–160, 2021.
- [40] Nagarajan VA, Selwin Rajadurai J and Anil Kumar T.: A digital image analysis to evaluate delamination factor for wind turbine composite laminate blade. *Compos: Part B* , Vol.43, pp.3153–3159, 2012.
- [41] Seehra, M., Narang, V., Geddam, U., & Stefaniak, A, correlation between x-ray diffraction and raman spectra of 16 commercial graphene-based materials and their resulting classification. *Carbon*, Vol.111, pp.380-385, 2017.
- [42] Norbert Geier, Karali Patra, Ravi Shankar Anand, Sam Ashworth, Barnabás Zoltán Balázs, Tamás Lukács, Gergely Magyar, Péter Tamás-Bényei, Jinyang Xu, J Paulo Davim.: A critical review on mechanical micro-drilling of glass and carbon fibre reinforced polymer (GFRP and CFRP) composites, *Composites Part B: Engineering*, Vol.254, 2023.
- [43] Pramod R, Basavarajappa S, Veeresh Kumar G, Chavali M.: Drilling induced delamination assessment of nanoparticles reinforced polymer matrix composites. *Proceedings of the Institution of Mechanical Engineers, Part C: Journal of Mechanical Engineering Science*, Vol.236(6), pp.2931-2948, 2022.
- [44] Su, F., Wang, Z., Yuan, J., & Cheng, Y., Study of thrust forces and delamination in drilling carbon-reinforced plastics (cfrps) using a tapered drill-reamer. *The International Journal of Advanced*

- Manufacturing Technology, Vol.80(5-8), pp.1457-1469, 2015.
- [45] Norbert Geier, J. Paulo Davim, Tibor Szalay.: Advanced cutting tools and technologies for drilling carbon fibre reinforced polymer (CFRP) composites: A review, *Composites Part A: Applied Science and Manufacturing*, Vol.125, 2019.
- [46] Geun Woo Kim, Kang Yong Lee.: Critical thrust force at propagation of delamination zone due to Drilling of F.R.P./metallic strips, *Composite Structures*, Vol.69, pp.137–141, 2005
- [47] Shrikant M. Harle.: Durability and long-term performance of fiber reinforced polymer (F.R.P.) composites: A review, *Structures*, Vol.60, 2024.
- [48] N.S. Mohan, A. Ramachandra, S.M. Kulkarni.: Influence of process parameters on cutting force and Torque during Drilling of glass–fiber polyester reinforced composites, *Composite Structures*, Vol.71, pp.407–413, 2005.
- [49] I.S. Shyha, S.L.Soo, D.K.Aspinwall, S.Bradley, R.Perry, P.Harden, S.Dawson.: Hole quality assessment following drilling of metallic-composite stacks, *International Journal of Machine Tools & Manufacture*, Vol.51, pp.569–578, 2011.
- [50] Soo SL, Abdelhafeez AM, Li M, Hood R, Lim CM.: The Drilling of carbon fibre composite–Aluminium stacks and its effect on hole quality and integrity. *Proceedings of the Institution of Mechanical Engineers, Part B: Journal of Engineering Manufacture*, Vol.233(4), pp.1323-1331, 2019.
- [51] Jing Liu, Deyuan Zhang, Long Gang Qin, Lin Song Yan, Feasibility study of the rotary ultrasonic elliptical machining of carbon fiber reinforced plastics (CFRP), *International Journal of Machine Tools & Manufacture*, Vol.53, pp.141–150, 2012.
- [52] V.I. Babitsky, V.K. Astashev, A. Meadows.: Vibration excitation and energy transfer during ultrasonically assisted Drilling, *Journal of Sound and Vibration*, Vol.308, pp.805–814, 2007.
- [53] Siroos Ahmadi, Afshin Zeinedini, Experimental.: theoretical and numerical investigation of the drilling effects on mode I delamination of laminated composites, *Aerospace Science and Technology*, Vol.104, 2020.
- [54] T.Panneerselvam, S.Raghuraman, T.K.Kandavel, K.Mahalingam.: Evaluation and analysis of delamination during Drilling on Sisal-Glass Fibres Reinforced Polymer, *Measurement*, Vol.154, 2020.
- [55] Ergün Ekici, Ali Riza Motorcu, Ensar Yıldırım, An Experimental Study on Hole Quality and Different Delamination Approaches in the Drilling of CARALL, a New FML Composite, *FME Transactions*, Vol.49, pp.950-961, 2021.
- [56] Zhenyuan Jia, Chen Chen, Fuji Wang, Chong Zhang, Analytical study of delamination damage and delamination-free drilling method of CFRP composite, *Journal of Materials Processing Technology* Vol.282, 2020,
- [57] Sorrentino L, Turchetta S, Bellini C. A new method to reduce delaminations during Drilling of F.R.P. laminates by feed rate control. *Compos Struct*, Vol.186, pp.154–64, 2018.
- [58] Prakash M, Dileep Aditya Dhar P. Investigation on the effect of drilling parameters on the tool wear and delamination of glass fibre-reinforced polymer composite using vibration signal analysis. *Journal of Composite Materials*. Vol.52(12), pp.1641-1648, 2018.
- [59] Pramod, R., S. Basavarajappa, and G.B. Veeresh Kumar.: Investigation on Surface Roughness of Drilled Holes in Nanoparticle Filled Polymer Matrix Composites. *Advances in Science and Technology*, Vol.105, pp.68–76, 2021.
- [60] Wang F, Yin J, Ma J, Jia Z, Yang F, Niu B.: Effects of cutting edge radius and fiber cutting angle on the cutting-induced surface damage in machining of unidirectional CFRP composite laminates, *Int J Adv Manuf Technol*, Vol.91 (9-12) pp. 3107-3120, 2017.
- [61] Lissek F, Tegas J, Kaufeld M.: Damage quantification for the machining of CFRP: an introduction about characteristic values considering shape and orientation of drilling- induced delamination. *Procedia Eng*, Vol.149, pp.2–16, 2016.
- [62] Xu J, El Mansori M, Chen M, Ren F.: Orthogonal cutting mechanisms of CFRP/Ti6Al4V stacks, *Int J Adv Manuf Technol*, Vol.103 (9), pp. 3831-3851, 2019,
- [63] Altın Karataş M, Gökkaya H.: A review on machinability of carbon fiber reinforced polymer (CFRP) and glass fiber reinforced polymer (GFRP) Composite materials, *Def Technol*, Vol.14 (4), pp.318-326, 2018.
- [64] Boccarusso L, Fazio DD, Durante M, Langella A, Capece Minutolo FM.: CFRPs Drilling: comparison among holes produced by different drilling strategies, *Procedia CIRP*, Vol.79, pp. 325-330, 2019.
- [65] Durante M, Boccarusso L, Fazio DD, Langella A.: Circular cutting strategy for drilling of carbon fiber-reinforced plastics (CFRPs), *Mater Manuf Process*, Vol.34 (5), pp. 554-566, 2019
- [66] Ergün Ekici, Ali Riza Motorcu, Gültekin Uzun, Multi-Objective Optimization of Process Parameters for Drilling Fiber Metal Laminate Using a Hybrid GRAPCA Approach, *FME Transactions*, Vol. 49, 356-366, 2021.
- [67] A Caggiano, Machining of fibre reinforced plastic composite materials, *Materials (Basel)*, Vol.11, 2018.
- [68] Sakthivel, M., Vijayakumar, S. and Jenarthanam, M.P, Grey-fuzzy logic to optimize process parameters in drilling of glass fibre reinforced stainless steel mesh polymer composite, *Pigment & Resin Technology*, Vol. 46, No. 4, pp. 276-285.
- [69] Kumar, M., Gupta, R.K., Pandey, A., Goyal, R., Goyal, A. A Review on Processes of Fabrication



and Properties of Nano-hybrid Metal Matrix Composites. In: Yadav, S., Singh, D., Arora, P., Kumar, H. (eds) *Proceedings of International Conference in Mechanical and Energy Technology. Smart Innovation, Systems and Technologies*, Vol.174, Springer, Singapore, 2020.

- [70] T. Srinivasan, K. Palanikumar, K. Rajagopal, B. Latha, Optimization of delamination factor in drilling G.F.R.–polypropylene composites, *Mater. Manuf. Processes*, Vol.32 (2), pp. 226-233, 2017.
- [71] D. Vijayan, T. Rajmohan.: Modeling and evolutionary computation on drilling of carbon fiber-reinforced polymer nanocomposite: an integrated approach using R.S.M. based PSO, *J Brazilian Soc Mech Sci Eng*, Vol.41, 2019.
- [72] Kristof Starost, Evelien Frijns, Jo Van Laer, Nadimul Faisal, Ainhua Egizabal, Cristina Elizextea, Maria Blazquez, Inge Nelissen, James Njuguna.: Assessment of nanoparticles release into the environment during drilling of carbon nanotubes/Epoxy and carbon nanofibres/Epoxy nanocomposites, *Journal of Hazardous Materials*, Vol.340, pp.57-66, 2017.
- [73] Lipsamayee Mishra, Debadutta Mishra, Trupti Ranjan Mahapatra.: Optimization of process parameters in Nd:YAG laser micro-drilling of graphite/epoxy based polymer matrix composite using Taguchi based Grey relational analysis, *Materials Today: Proceedings*, Vol.62, Part 14, pp.7467-7472, 2022.
- [74] M.H. Kothmann, R. Zeiler, A. Rios de Anda, A. Brückner, V. Altstädt, Fatigue crack propagation behaviour of epoxy resins modified with silica-nanoparticles, *Polymer*, Volume 60, Pages 157-163, 2015.

- [75] Shivi Kesarwani, Rajesh Kumar Verma, S.C. Jayswal, Evaluation of the cutting force, burr formation, and surface quality during the machining of carbon nanoparticle modified polymer composites for structural applications, *Materials Today Communications*, Vol.34, 2023.

---

**ИСТРАЖИВАЊЕ УТИЦАЈА ДЕЛАМИНАЦИЈЕ  
ИЗАЗВАНЕ БУШЕЊЕМ И ХАБАЊА АЛАТА  
НА ПРЕОСТАЛУ ЧВРСТОЋУ У  
ПОЛИМЕРНИМ НАНОКОМПОЗИТИМА**

**Р. Прамод, Г.Б.В. Кумар, С. Басаварацана**

Раслојавање изазвано бушењем, ломови, одвајање, хабање алата и расплињавање матрице смањују заосталу чврстоћу полимерних композита. Новина ових студија лежи у укључивању нано-пунила графена и монтморилонит глине са 2% тежинског процента за матрицу за очвршћавање како би се минимизирала заостала напрезања изазвана бушењем и хабање алата. Комбиновање термичких и механичких својстава матрице са влакнима смањује макро и микро преостала напрезања влакнастог композита. Интерламинарна чврстоћа на смицање је порасла за 16%–23% и жилавост лома за 22% коришћењем нанопунила, минимизирајући раслојавање пукотина изазвано бушењем и погоршање затезне чврстоће композита. Нанопунила су повећала задржавање затезне чврстоће ламината и време до отказивања. Фактори хабања алата и деламинације порасли су на излазу рупе са повећаним избушеним рупама, али су побољшани на улазу за 16%. Ова студија показује замршену везу између састава композитног материјала, варијабли процеса и структурног интегритета у композитима изложеним бушењу.